Heliyon

ELSEVIER

Received:
8 April 2016
Revised:
6 September 2016
Accepted:
7 September 2016

Heliyon 2 (2016) e00157

Resolving spatiotemporal characteristics of the seasonal hypoxia cycle in shallow estuarine environments of the Severn River and South River, MD, Chesapeake Bay, USA

Andrew C. Muller [a,*], **Diana L. Muller** [b], **Arianna Muller** [c]

[a] *United States Naval Academy, Oceanography Department, Annapolis, Maryland 21402, USA*

[b] *Center of Applied Technology-North, Severn, Maryland 21144, USA*

[c] *Brevard College, Brevard, North Carolina 28712, USA*

* Corresponding author.

E-mail address: amuller@usna.edu (A.C. Muller).

Abstract

The nature of emerging patterns concerning water quality stressors and the evolution of hypoxia within sub-estuaries of the Chesapeake Bay has been an important unresolved question among the Chesapeake Bay community. Elucidation of the nature of hypoxia in the tributaries of the Chesapeake Bay has important ramifications to the successful restoration of the Bay, since much of Bay states population lives within the watersheds of the tributaries. Very little to date, is known about the small sub-estuaries of the Chesapeake Bay due to limited resources and the difficulties in resolving both space and time dimensions on scales that are adequate to resolve this question. We resolve the spatio-temporal domain dilemma by setting up an intense monitoring program of water quality stressors in the Severn and South Rivers, MD. Volume rendered models were constructed to allow for a visual dissection of the water quality times series which illustrates the life cycle of hypoxia and anoxia at the mid to upper portions of the tidal tributaries. The model also shows that unlike their larger Virginian tributary counterparts,

http://dx.doi.org/10.1016/j.heliyon.2016.e00157

there is little to no evidence of severe hypoxic water intrusions from the main-stem of the Chesapeake Bay into these sub-estuaries.

Keywords: Earth sciences, Hydrology

1. Introduction

Estuaries and their adjacent coastal environments are an ecologically diverse, dynamic, and critical to many aquatic species. These marginal marine zones lie at the intersection of terrestrial and marine environments leaving them highly vulnerable to pollutant loads [1, 2, 3]. One of the major consequences of combining vulnerable waterways with increased pollutant pressures is the realization that the health of many estuarine environments has been declining as recognized by the growth of "dead zones" [4]. Severe hypoxia, defined as dissolved oxygen less than 62.5 μM (2.0 mgl^{-1}), and anoxia have been increasing in both their spatial and temporal extent over the last several decades leading to numerous deleterious consequences to these marginal marine environments [5, 6, 7, 8]. These effects include decreased acreage of submerged aquatic vegetation (SAV) as result of the production of hydrogen sulfide in anoxic water which then invades roots and rhizomes of the SAV causing a potential die-off [9], disruptions in estuarine food webs [10], loss of invertebrate and vertebrate species [11, 12, 13] and increases in harmful algal blooms (HAB) occurrences [14, 15, 16].

Although the primary biogeochemical and physical causes have been attributed mainly to overly eutrophic conditions, meteorological events [17, 18, 19, 20] coupled with summer-time water column stratification, the timing and full extent in many areas is still not fully resolved [21, 22, 23, 24, 24, 25]. This is especially true for the smaller tidal tributaries of large estuarine systems such as the Chesapeake Bay [26]. Resolving the complete spatio-temporal evolution of water-quality indicators has also become critically important to the documentation of adaptive management effectiveness in coastal settings such as the total maximum daily load (TMDL) strategy or nutrient pollution diet instituted by the EPA Chesapeake Bay Program [27]. Some of the most important unresolved questions include "how does the timing and evolution of hypoxia and anoxia within tributaries of an estuarine system relate to the parent estuary and if the main physio-chemical processes leading to the development of hypoxia is rooted within the tributary or the parent estuary?"

As a result, there has been increased attention towards developing coastal observing systems. These observing systems or networks are increasing our knowledge of the spatial and temporal variability in the coastal zone and are fueling recent advances in coastal zone modeling. With the realization of the high degree of variability in these areas coupled with concerns over climate change, it has now become apparent that better visualization tools are needed to fully resolve

http://dx.doi.org/10.1016/j.heliyon.2016.e00157

the spatio-temporal nature of water quality variables in these dynamic environments from both observing system data and model outputs [28, 29, 30, 31]. Visualization of coastal observing systems and applied numeric modeling techniques in estuaries usually constitutes problems in the space-time domain. Space-time as a single continuum needs to be in the same fabric for a complete analysis. This concept of a space-time continuum leads to the spatiotemporal dilemma. Several attempts have been made to resolve the nature of water quality parameters, however they are often observed in space or in time with little attempt to combine these dimensions [32, 33, 34, 35, 36]. This is mainly due to the dilemma that faces all physiochemical-observing programs, either a program is spatially intensive or it is temporally intensive, but usually not both. Continuous monitoring instrumentation has afforded the availability of higher resolution in the temporal domain, but there are relatively few locations and it is only in one spatial dimension. The key is to find a way to add at least two spatial dimensions (horizontal and vertical) with time. The main obstacles to translating physiochemical parameters into the spatiotemporal dimension include cost, data integration, and the lack of data visualization tools. It is cost prohibitive to set up continuous monitoring instrumentation over a large region and in multiple spatial dimensions. Conversely, it is difficult to stitch together continuous monitoring data taken at a few locations with more intense spatial data taken at multiple time scales. Although a number of studies have suggested that kriging is a preferable method for data interpolation of water quality variables in estuarine environments [37, 38, 39], adding the temporal dimension poses a number of problems [40].

The focus of this research was to create volume rendered models of water quality stressors in shallow tributaries of the Chesapeake Bay in order to resolve the timing, duration, and extent of hypoxia and anoxia in these environments. This method fulfills a unique niche for time series analysis using a visual dissection of the water column for the physiochemical parameters. Most times series studies involve one spatial dimension, other studies examine slices of the water column in two spatial dimensions, and Bever et al. (2013) utilizes model simulations to calculation potential hypoxic volume days.

This research addresses the following key questions: 1) what is the space-time evolution of hypoxia within small tidal tributaries within the Chesapeake Bay system? 2) Does bottom water hypoxia and anoxia develop within the tidal tributary or are the severe hypoxic-anoxic water masses transported into the small tributaries from the main channel of the Chesapeake Bay? 3) Does shallow water hypoxia behave in a similar fashion in large tributaries as compared to shallow tributaries? In order to answer these important questions, we applied the direct volume rendering technique to physicochemical parameters measured over multiple spatial and temporal scales in shallow tributaries of the Chesapeake Bay. Despite its advantages in imaging three-dimensional data, volume rendering

http://dx.doi.org/10.1016/j.heliyon.2016.e00157

is rarely if ever used in the coastal and estuarine research community [29]. Another main goal of this study is to introduce the direct volume rendering technique and its powerful capabilities to the community of estuarine scientists and managers.

2. Materials and methods

2.1. Study area

The study area includes the tidal portions of the Severn and South Rivers, which are tributaries of the Chesapeake Bay, located on Maryland's Lower Western Shore (Fig. 1). The South and Severn Rivers have numerous tidal creeks forming a typical dendritic pattern that resembles most low sediment discharge coastal plain estuaries. The bathymetry of the Severn and South Rivers are similar by the fact each river contains a deeper middle section, with shallower mouths and headwaters. These rivers are different in that the Severn River is deeper at the mouth and about 5 meters deeper at its mid-section vs South River. In the Severn River there is a unique bowl shaped geomorphic feature, this is called Round Bay and is represented by stations RBS (Round Bay South), SRN 5 (middle section of Round Bay), and RBN (Round Bay North). A shallow sill exists at either end of Round Bay constricting flow in the area. Located at the mouth of both rivers shallow sills exist.

Each river's watersheds are examples of classic urban/suburban communities, both containing approximately 66,000 residents in each watershed. These sub-estuaries are oriented northwest to southeast and are between 15 and 18 kilometers long. The

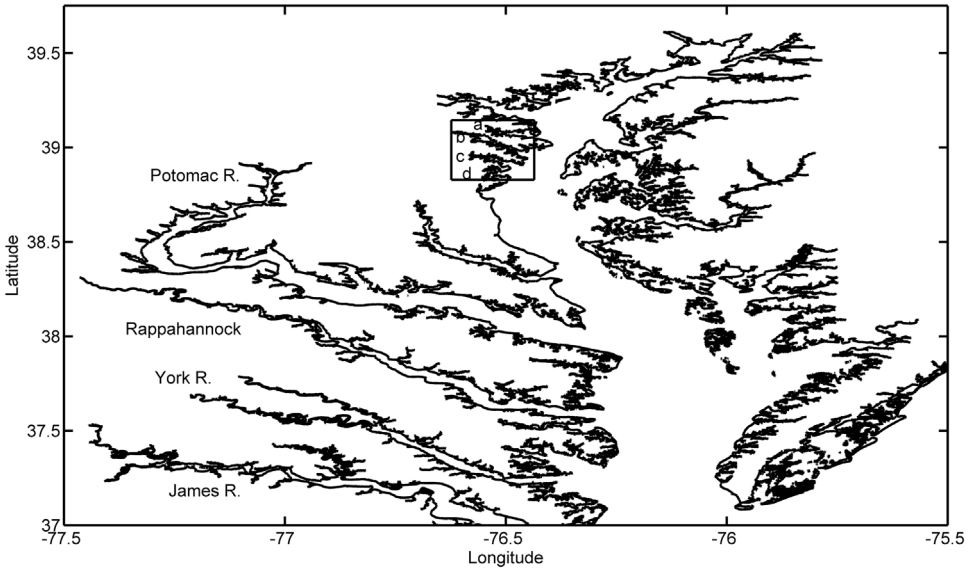

Fig. 1. Location of the Lower-Western shore tributaries of the upper Chesapeake Bay, which contains the Magothy (a), Severn (b), South (c) and Rhode-West Rivers (d).

http://dx.doi.org/10.1016/j.heliyon.2016.e00157

South and Severn Rivers are classified as mesohaline environments with salinities ranging from 10–12 at the mouth to 4–7 at their headwaters. The Lower Western Shore tidal tributaries of the Chesapeake Bay are also characterized by low freshwater inputs, which drive small salinity gradients resulting in weak partially-mixed to well mixed systems with low flushing rates. Tides are classified as micro tidal with a range of approximately 0.3 meters [3, 41]. Land use and shoreline attributes of each watershed are shown in Table 1.

2.2. Field methods

A detailed monitoring program in both the spatial and temporal dimensions was first developed for each estuary. In the Severn River, nine main channel stations were monitored on a weekly basis, while seven stations were monitored in the South River. Vertical profiles were taken weekly for dissolved oxygen, temperature, and salinity in the Severn River, while pH, and chlorophyll *a* were added to the above parameters in the South River. The sampling period took place from late May through September (2010–2014) at each of the 16 locations as shown in Fig. 2. YSI (Yellow Springs Instruments Inc. 556 and/or Hydrolab DS5 sondes were used for the monitoring programs. The instruments were calibrated pre and post monitoring events as per manufacturer's guidelines and the Chesapeake Bay Program monitoring QA/QC protocol document. Station distances were normalized to the station at the mouth at each river. For the Severn River, the station that represents the mouth opening up to the Chesapeake Bay proper is

Table 1. Comparison of Severn and South Watersheds for land-use and shoreline attributes.

Severn River Watershed	*South River Watershed*
177 km^2 total watershed land	146 km^2 total watershed land
245 km of streams	396 km of streams
Urban 38%	Urban 39%
Agricultural Land 10%	Agricultural Land 15%
Forest 32%	Forest 30%
Wetland <1%	Wetland <1%
Impervious (roads, parking lots) 19%	Impervious (roads, parking lots) 15%
Shoreline length 70 km	Shoreline length 60 km
Tidal water surface area 23.5 km^2	Tidal water surface area 16.4 km^2
Tidal water volume 165 km^3	Tidal water volume 82 km^3
Living shoreline 7%	Living shoreline 13%
Hardened shoreline 43% (bulkhead, concrete, rocks)	Hardened shoreline 47% (bulkhead, concrete, rocks)

http://dx.doi.org/10.1016/j.heliyon.2016.e00157

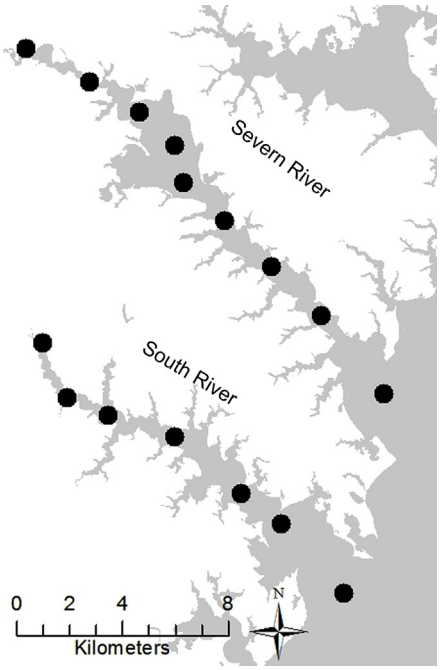

Fig. 2. Sample locations in the Severn and South Rivers, MD.

station SRN 0, while station MS 1 represents the mouth of the South River. Average distances from the mouth of the river and depths are listed in Table 2 and Table 3 for the Severn and South Rivers respectively. Station depths were recorded using a Hummingbird Helix 9 DI Sonar GPS unit mounted to the vessel used to collect samples longitudinally throughout each sub-estuary.

Table 2. Severn River station distances normalized to station SRN 0, average depths and location.

Station	Distance from mouth (km)	Average depth (m)	Lat., Long.
SRN 0	0.0	6.0	38.9636, −76.4556
SRN 1	1.0	6.5	38.9902, −76.4828
SRN 2	3.7	6.5	39.0068, −76.5046
SRN 3	8.3	12.0	39.0225, −76.5250
RBS	10.2	7.5	39.0357, −76.5427
SRN 5	11.5	7.0	39.0482, −76.5465
RBN	13.5	8.0	39.0597, −76.5618
SRN 6	15.4	5.0	39.0702, −76.5833
SRN 7	18.0	1.5	39.0814, −76.6112

http://dx.doi.org/10.1016/j.heliyon.2016.e00157

Table 3. South River station distances normalized to station MS 1, average depths and location.

Station	Distance from mouth (km)	Average depth (m)	Lat., Long.
MS 1	0.0	4.5	38.895678, −76.473597
MS 1A	3.7	6.5	38.919578, −76.500936
MS 1B	5.4	6.0	38.929831, −76.518374
MS 2	8.7	8.0	38.949213, −76.546948
MS 3	11.1	5.0	38.956675,-76.575850
MS 4	12.9	3.0	38.962661,-76.593797
MS 5	15	2.0	38.981264,-76.604544

2.3. Volume rendering

Direct volume rendering (DVR) is a visualization technique used to display three-dimensional scientific data. In this technique, images are directly produced using voxels from scalar datasets via the function f (x,y,z). Direct volume rendering techniques began in the early 80's primarily in the medical field in order to extract more information from CT and MRI scans. Despite its common use in the medical industry and its significant advantages in visualization of complex images, the environmental sciences do not typically use the DVR technique. This technique essentially treats data as a semi-transparent medium that emits, transmits and absorbs light. As a result, the observer is able to "see" through the data or look inside the media. The primary advantage of this technique is its flexibility, given that the method allows the researcher to rotate the image highlighting areas of interest. In this case the technique allows the researcher to look inside the estuary in order to gain insight into the development of water quality parameters in space and time as well as the processes involved in the evolution of the water quality stressors mapped [42, 43].

Since the DVR method treats data as a transparent medium, Eq. (1) can be used to calculate the intensity of light as a ray of light passes through the volume.

$$I(D) = I0e^{-\int_0^D p(t)\,Adt} + \int_0^D C(s)\,p(s)\,Ae^{-\int_0^D p(t)\,Adt}\,ds \quad (1)$$

In Eq. (1), s represents position and is equal to zero at the volume edges and D at the eye. A represents the area and ρ is the density per unit. C is the emissive glow per unit area projected. In order to create three-dimensional images, the DVR technique produces a stack of two-dimensional slices incrementally. Therefore, the discretized form of Eq. (1) is typically used. This is accomplished by using a Riemann sum as expressed in Eq. (2) [42, 43, 44].

http://dx.doi.org/10.1016/j.heliyon.2016.e00157

$$I(D) \approx I0 \prod_{i=1}^{n} ti + \sum_{i=1}^{n} gi \prod_{j=i+1}^{n} tj \tag{2}$$

In the above equation, ti and gi are defined as follows: $ti = e^{-\rho(i\Delta\chi)A(\Delta\chi)}$, $gi = C(i\Delta\chi)\rho(i\Delta\chi)A$

Algorithms for direct volume rendering are broken down into three main steps. Step 1 is sampling, step 2 is classification and step 3 is compositing. A detailed description of the ray casting method used in direct volume rendering can be found in Johnson et al. (2004), Mak et al. (2011), Callahan et al. (2008), and Engle et al. (2001) [42, 43, 44, 45].

2.4. Spatiotemporal model construction

Volume rendered models of hypoxia, temperature, salinity and Chl-*a* (Chlorophyll-*a*), were constructed using the commercial product Voxler 3.0 from Golden software [46]. In all the models presented in this paper, the X-axis represents time in Julian weeks, while the Y-axis is the normalized distance in km from the mouth of estuary taken at either station SRO (Severn River), or MS1 (South River). Julian week 1 is the first week in January, while Julian week 52 is the last week in December of a given year. Depth in meters is represented by the Z-axis, which is rotated to yield positive values from the surface down to the bottom. Bathymetry for each estuary was based on average depths measured at each station. Station depths were then gridded using an inverse distance isotropic second order scheme, and simulated as a height field for each river (Fig. 3). Each data file used to generate a particular volume rendered model had a minimum of 1000 rows. Input parameters such as distance, Julian week, depth, and concentration (dissolved oxygen) were first gridded using an inverse distance isotropic scheme to the second

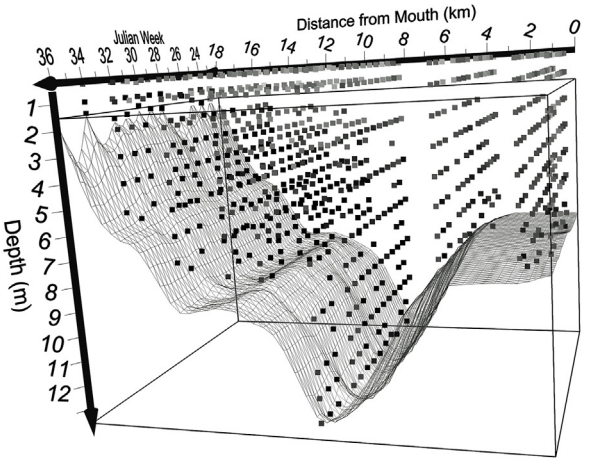

Fig. 3. Sample model construction for volume rendering. The X- axis is the normalized distance from the mouth of the river, Y represents time in Julian weeks and z is the depth. Circles represent location of actual samples, and the mesh is the average bathymetry of the river.

http://dx.doi.org/10.1016/j.heliyon.2016.e00157

power. All volume rendered models used the 3-D texture method with 400 slices. Alpha blending was used for compositing and a trilinear scheme was employed for sampling. The opacity is then set for each individual model to display the features of interest [47]. In this cast, we are able to examine water quality slices with time through the estuary in order to reveal space-time patterns of physicochemical parameters such as dissolved oxygen, salinity, and temperature.

Once the spatiotemporal model of a particular parameter is created, it is then possible to determine the spatiotemporal volume of the parameter in question. Since time is treated as a spatial dimension, we determined the volume of the river property by first creating a rendered isosurface of a specific parameter. The volume above or below each isosurface is then calculated by multiplying the distance (X) in km, by the depth (Z) in km and the time (Y) in weeks to yield a volume for the given parameter with units of km^2w.

2.5. Seasonal cycle assessment of physiochemical parameters

The spatiotemporal life cycle assessment of water quality parameters is critically important to the understanding and assessment of ecological sustainability. As a result, in order to assess the sustainability of these small tributary systems in relation to hypoxia and anoxia we adopted the dissolved oxygen criterion developed by the United States Environmental Protection Agency's (USEPA) Chesapeake Bay Program. The USEPA defines shallow water tributaries such as the South and Severn Rivers as having an open water use designation. For open water systems, the USEPA defines 5.0 mgl^{-1} as the sustainable level for living resources and hypoxic conditions below this level. Severe hypoxia is defined in this paper, as dissolved oxygen values below 2.0 mgl^{-1}, while anoxia is defined operationally as values below 0.2 mgl^{-1} [48]. Using the volume rending technique the method allows for the calculation of hypoxic volume in weeks.

The direct volume rendering method was applied to temperature and salinity for examination of patterns. Temperature threshold was based on a value intermediate to those critical to many living resources in the Chesapeake Bay [48], and salinity greater than five is an important boundary classifying oligohaline from mesohaline conditions important to the biology and ecology of estuaries [49]. Temperature is also an important water quality stressor, for it affects dissolved oxygen concentrations via decreased solubility with rising values and helps to fuel large algal blooms that also decrease oxygen concentrations. Several studies have also shown that many of the historically important species in the Bay have a thermal tolerance as well. This includes living resources such as rockfish (24 °C), Yellow Perch (25 °C) and SAV (submerged aquatic vegetation, 29 °C). As a result, we also determined the spatiotemporal volume at and above the 29 °C isosurface [50, 51, 52, 53, 54, 55, 56, 57].

http://dx.doi.org/10.1016/j.heliyon.2016.e00157

3. Results

3.1. Spatiotemporal life cycle and assessment of hypoxia

The direct volume rendering model (DVR) uses four parameters, with two spatial, one temporal and one concentration as a voxel. The interpretation of the DVR models shows the horizontal axis (x) is the longitudinal distances from the mouth of the tidal river, as 0 km going toward the headwaters as 18 km for Severn River and 15 km for South River, this is considered the space domain. The vertical axis (z) is depth in meters and is the second space domain, and time is "marching" out of the page on the y-axis, displayed in Julian weeks, is the temporal domain. The concentration of the physiochemical parameters are rendered as voxels and color-coded to concentrations.

The life cycle of hypoxia in the Severn River tidal estuary in 2010, (Fig. 4) indicates that the dissolved oxygen volumes are at or above 5 mgl^{-} at the mouth of the Severn River (0 km). During weeks 18 to 26 moving upstream at distances at 4 km toward distance 18 km, the dissolved oxygen volumes become hypoxic from the bottom to a depth of 4.5 meters. At weeks 28 to 36, the hypoxic volume increases in distance and expands to a depth of 1-meter. Anoxic conditions developed at distance 12 km at weeks 30 to 36 at a depth of 8 m and continued upstream to 18 km to a depth of 1 meter. The calculations show that 18% was 5 mgl^{-} or greater and 61% was less than 2 $mgl^{-1,}$ and 4% was 0.2 $mgl^{-1.}$ This figure directly shows the life cycle of hypoxic volume spreading vertically, horizontally, and temporally through the water column and indicates the hypoxic waters are not being imported into the Severn River (0 km) from the Chesapeake Bay.

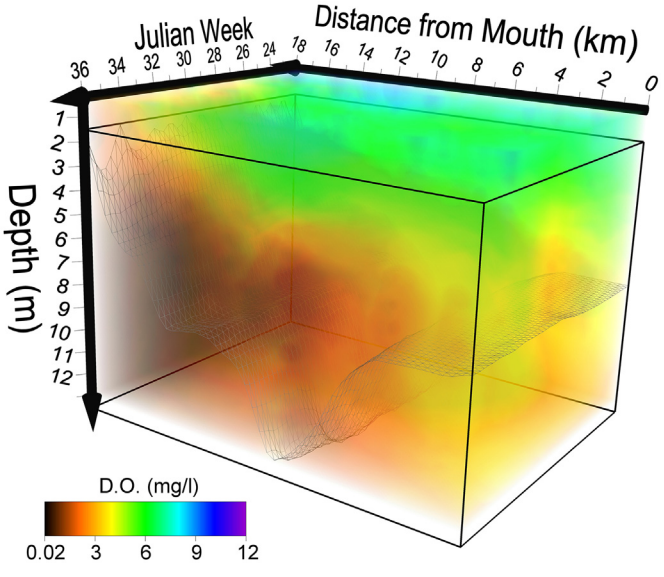

Fig. 4. Spatiotemporal model of of hypoxia in the Severn River 2010.

http://dx.doi.org/10.1016/j.heliyon.2016.e00157

The South River DVR model for dissolved oxygen indicates that the volume is 5.0 mgl^{-1} or better at the mouth for the entire life cycle of 2010 (Fig. 5). The spatiotemporal severe hypoxia does not develop until week 30 at a distance of 10 km at a depth of 5 m. Anoxia develops primarily in the deep-water section near 9 km. The spatiotemporal hypoxic volume showed that 71% of the was at or above the 5 mgl^{-1}, while 14% was below the 2.0 mgl^{-1}, 7.2% was at 2 mgl^{-1}, and 0.02% for 0.2 mgl^{-1}.

The 2011 DVR spatiotemporal model for the Severn River at 0 km to 8 km is at or above 5 mgl^{-1} (Fig. 6). At distances 2 to 6 km the dissolved oxygen volume become hypoxic from 5 m to 9 m (bottom) at week 26 through 28, then increasing during the year. At distances of 12 to 18 km the evolution of hypoxic conditions are found at weeks 28 to 36 at the bottom (5 m) coming up to the surface (1m). Anoxic volume are located at distance of 14 to 18 km from weeks 28 to 36 from the bottom (9 m) coming up to the surface (1 m). The spatiotemporal hypoxic volume calculated was 28.5% for 5 mgl^{-1}, 44.5% for 2.0 mgl^{-1}, and anoxic volume as 27% for 0.2 mgl^{-1}. The anoxic volume is located in the shallows of the Severn River and is not only located in the main channel deep sections. This DVR of the Severn River shows that no Chesapeake Bay hypoxic or anoxic water is entering the sub-estuary and that the hypoxic-anoxic conditions develop within this tidal creek.

Conversely, the DVR model for the South River in 2011 shows dissolved oxygen between 0 km to 15 km from weeks 15 to 25 the dissolved oxygen is at or above 5 mgl^{-1} (Fig. 7). Spatiotemporal hypoxia is found during weeks 25 to 40 only toward the bottom depth. The spatiotemporal dissolved oxygen volumes calculated was

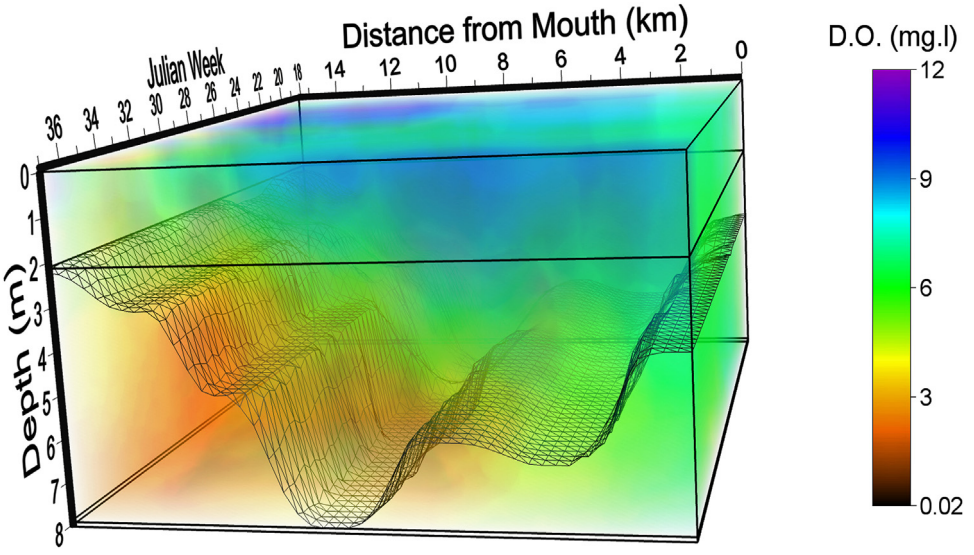

Fig. 5. Spatiotemporal model of hypoxia in the South River 2010.

http://dx.doi.org/10.1016/j.heliyon.2016.e00157

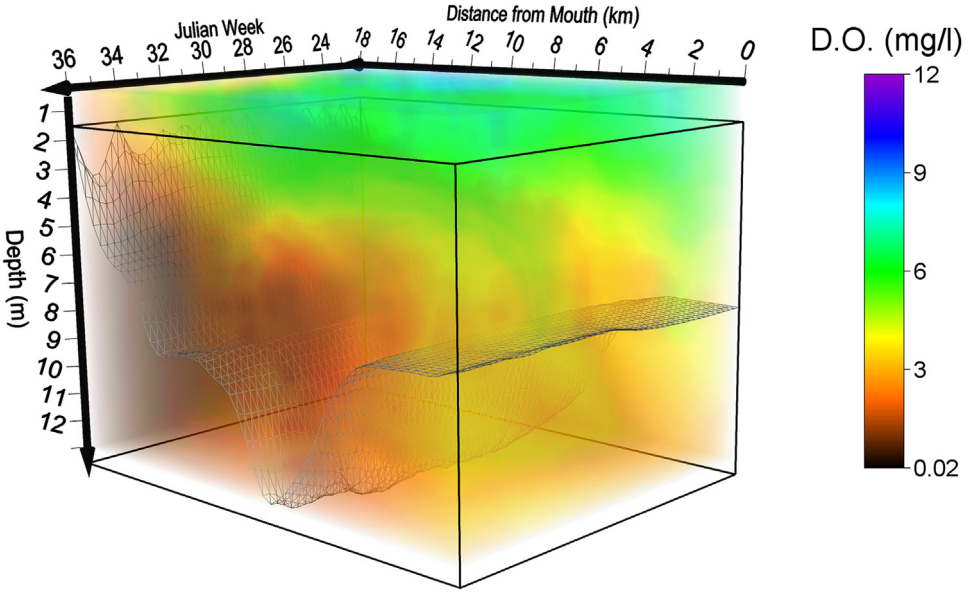

Fig. 6. Spatiotemporal model of hypoxia in the Severn River 2011.

92.6% at or above 5 mgl^{-1}, 7% for 2 mgl^{-1}, and 0.32% for 0.2 mgl^{-1}. The South River did not have any evidence of hypoxic water entering from the Chesapeake Bay, and the hypoxic conditions that evolved were localized within this system.

In order to capture a the complete life cycle of hypoxia within the small tributaries, monitoring in the South River began in early January of 2012. The spatiotemporal model for 2012, clearly indicates hypoxic conditions began around Julian week 18 and expand and contract throughout the water column until week 40. At week 40,

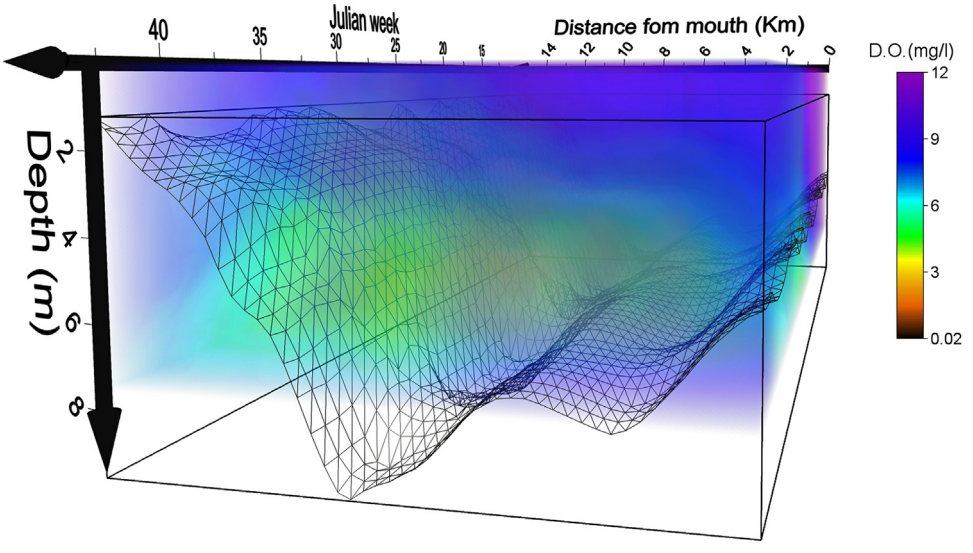

Fig. 7. Spatiotemporal model of hypoxia in the South River 2011.

http://dx.doi.org/10.1016/j.heliyon.2016.e00157

mixing is the dominant processes and the hypoxia has disappeared (Fig. 8). Also important to note is that the hypoxic condition in the river only reaches the upper and middle portions of the river (9 km). Hypoxia is absent throughout the water column including bottom water for almost 8 km into the river from the mouth. The spatiotemporal hypoxic volume calculated was 88% for 5.0 mgl^{-1}, 12% for 2 mgl^{-1}.

The DVR models for 2013 and 2014 in the Severn and South River showed a decrease in hypoxia and temperature. The results are found in Table 4.

3.2. Spatiotemporal life cycle of temperature and salinity

Since both temperature and salinity could cause dissolved oxygen deficits, the life cycle of these parameters were examined. The water column in the Severn River begins to heat significantly in the late spring around Julian week 22 or the last week of May. Temperatures tend to be cooler near the mouth of the river and much warmer near the headwaters, which is typical for estuarine systems during this time of the year [58]. During the 2010 season, temperatures rose to 29 °C and above in Round Bay between Julian weeks 29 and 33. The Severn River appears to be well mixed with respect to temperature at the mouth with growing stratification in the middle and upper reaches. Thermocline depths in the middle and upper parts of the river are between 3 to 5 meters, and lower at the headwaters. Maximum surface temperatures approached 31 °C in mid-July, while typical bottom temperatures were around 24 °C. Temperatures decrease down to approximately 25 °C by mid-September as mixing due to increasing storm intensity eroding the thermocline. Fourteen percent of the spatiotemporal volume lies at or above the 29 °C isosurface for the Severn River during 2010 (Fig. 9), while 10 percent of the spatiotemporal volume was below 24 °C. In 2011, the Severn River displayed a 10 percent decrease in the spatiotemporal volume at or above the 29 °C isosurface.

The South River displays many similarities with the Severn with respect to temperature, especially in the temporal domain. However, the South River is shallower than the Severn which allows for greater mixing. Surface temperatures

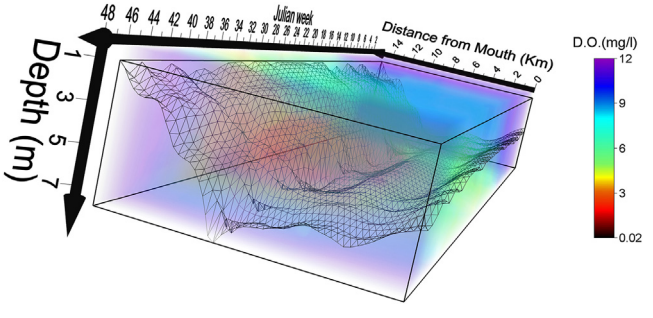

Fig. 8. Spatiotemporal model of hypoxia in the South River 2012.

http://dx.doi.org/10.1016/j.heliyon.2016.e00157

Table 4. Annual Spatiotemporal assessment of water quality in the Severn and South Rivers, May–September, 2010–2014.

		Spatiotemporal seasonal value (km^2*weeks)			
Sub-estuary	Year	Hypoxia < 5 mg/L	Hypoxia < 2 mg/L	Temperature >29 °C	Salinity >5
Severn River	2010	$2.6*10^3$	$1.5*10^3$	$4.1*10^1$	$3.2*10^3$
	2011	$3.1*10^3$	$1.2*10^3$	$1.2*10^{-1}$	$4.4*10^3$
	2012	$3.3*10^3$	$1.3*10^3$	1.6*10°	$4.9*10^3$
	2013	$4.0*10^3$	$2.2*10^1$	$2.3*10^{-1}$	$4.0*10^3$
	2014	NA	NA	NA	NA
South River	2010	$6.6*10^2$	$1.7*10^2$	$1.8*10^2$	$2.3*10^3$
	2011	$9.8*10^2$	11.7*10°	5.8*10°	$2.5*10^3$
	2012	$1.4*10^3$	$1.6*10^2$	$1.3*10^2$	$1.9*10^3$
	2013	$2,0*10^3$	6.7*10°	$5.0*10^{-1}$	$1.6*10^3$
	2014	$2.5*10^3$	$1.7*10^1$	8.2*10°	$1.2*10^3$

reached 33 °C in mid-July. Unlike the Severn River, stratification is weak at best and usually only forms around the middle potion of the river. Vertical mixing is strongest at the mouth in both the Severn and South Rivers. Horizontal temperature gradients in the South River are also similar to the Severn's in that the coolest temperatures are located at the mouth and the warmest temperatures are found at the headwaters. In 2010, 30 percent of the spatiotemporal value for temperature was at or above the 29 °C isosurface (Fig. 10). However, this value dropped substantially to 7 percent in 2011.

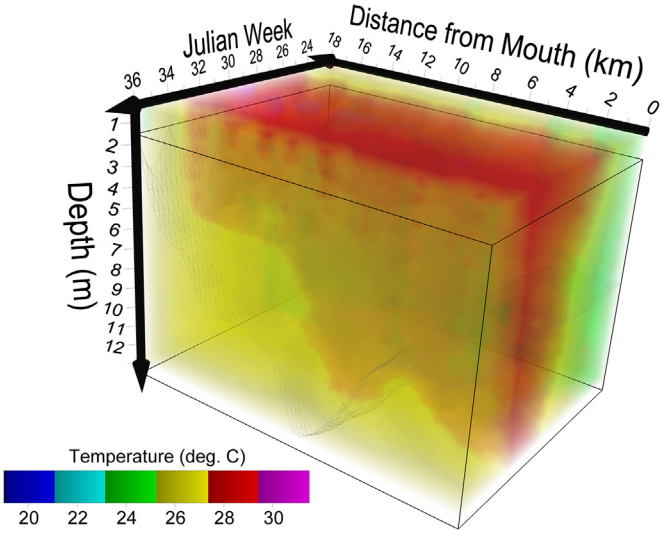

Fig. 9. Spatiotemporal model of temperature in the Severn River 2010.

http://dx.doi.org/10.1016/j.heliyon.2016.e00157

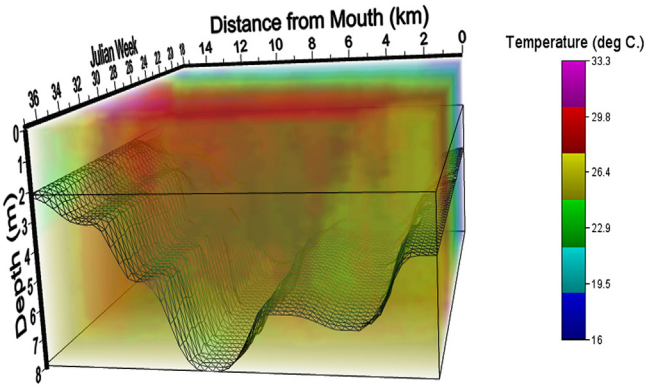

Fig. 10. Spatiotemporal model of temperature in the South River 2010.

The spatiotemporal direct volume rendering (DVR) model shows weak to moderate stratification, especially in the deeper sections of the Severn River, with a halocline between 3–5 meters. The surface freshwater input into the Sever River does not extend far into this portion of the tidal system. Hence, this drives a very weak salinity gradient causing a weak circulation resulting in a partially mixed to well mixed estuary depending on the time of the year and position within the estuary (Fig. 11). The temporal DVR pattern shows that salinity increase over time through the late spring into early fall (9–10 PSU)

Salinity in the South River exhibits similar trends, but experiences greater mixing in part due to its shallower depths. The South River is mostly well mixed with respect to salinity over most of the River with occasional slight stratification occurring during the spring in the upper regions (North River outflow, 15 km) and

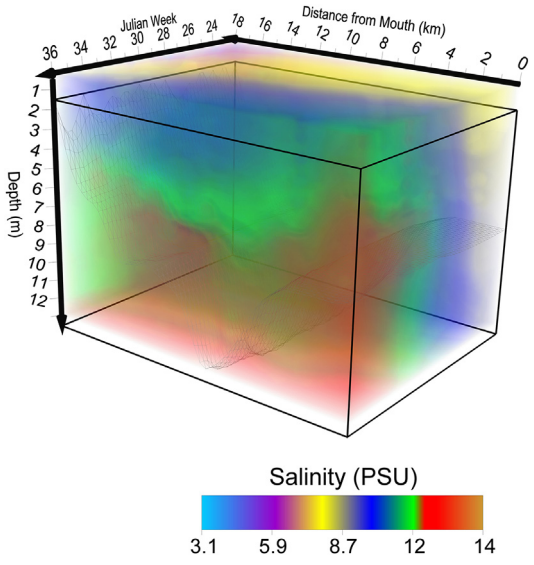

Fig. 11. Spatiotemporal model of salinity in the Severn River 2010.

http://dx.doi.org/10.1016/j.heliyon.2016.e00157

in the middle potion at the deepest spot (9 km) during late July to early August (Fig. 12). Weak surface horizontal salinity gradients dominate over vertical gradients driving a weak circulation system with an approximate 11-day flushing rate [3].

4. Discussion

Severe hypoxia and anoxia develop in both the Severn and South Rivers mainly in the deep middle sections and the very shallow up river sections close to the headwaters, and were not found in either of their estuarine river mouth. The DVR models clearly illustrate that there is no evidence of severe hypoxic or anoxic water masses intruding into these tributaries from the main-stem of the Chesapeake Bay. In contrast, Kou et al. (1991) found that the larger sub-estuarine river systems in the southern portion of the Chesapeake Bay watershed did show evidence of hypoxic waters entering the river mouths, and higher dissolved oxygen concentrations at the headwaters. This was due to the fact these estuarine river systems have deep trenches located at the at their mouths, which allows for the Chesapeake Bay anoxic water to enter [59, 60, 61, 62]. This is opposite to our finding in the smaller tidal tributaries of the northern Chesapeake Bay estuarine river systems. The South and Severn River systems both have shallow sandy sills at the estuarine river mouths and deeper riverine bottoms in the middle of the system. This structure physically prevents the anoxic Chesapeake Bay water from entering the South and Severn River systems. As further evidence for the lack of severe hypoxia entering the Severn River a monitoring transect was performed on August 18, 2010 in the Severn River's headwaters to the middle of the Chesapeake Bay (Fig. 13). In addition to the DVR models, this transect confirmed that hypoxia was found in the upper and mid sections of the Severn River, well oxygenated water at

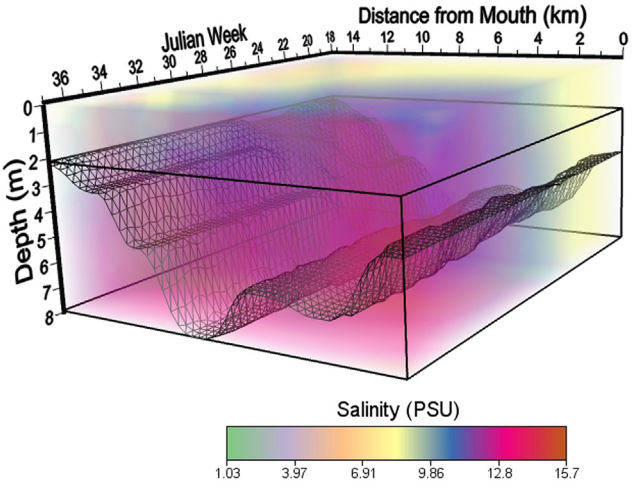

Fig. 12. Spatiotemporal model of salinity in the South River during 2010.

http://dx.doi.org/10.1016/j.heliyon.2016.e00157

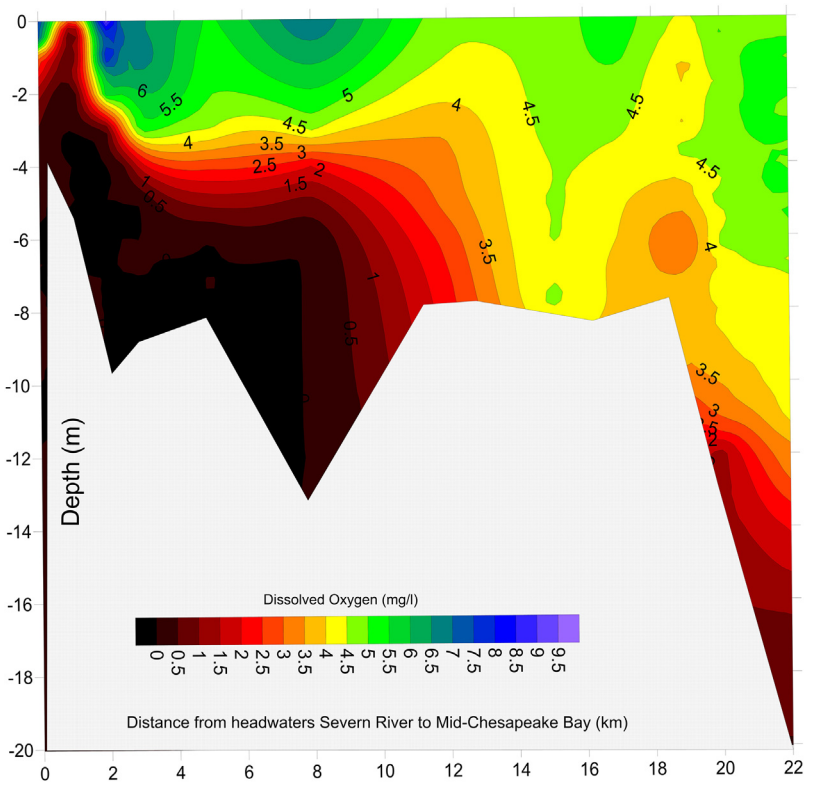

Fig. 13. Severn River to mid-Chesapeake Bay transect for dissolved oxygen, 2010.

the Severn River mouth, and hypoxic-anoxic waters in the main stem of the Bay. Further indicating a disconnect between the shallow water estuarine river systems and the main stem of the Chesapeake Bay. This realization is critically important, because it indicates that hypoxia and anoxia develops within the tributary separate from the parent Chesapeake Bay estuary [61].

The DVR models of the South and Severn Rivers provide valuable insight into the inner biophysical processes that control estuaries, especially the timing and development (life-cycle) of hypoxia and anoxia. Results from the temperature and salinity DVR models indicates that unlike Chesapeake Bay, these small tributaries are mainly dominated by temperature rather than salinity, and thus their density driven circulation and biological process are coupled via temperature. This is in contrast to the classic Pritchard type estuary that defines the Chesapeake Bay, and suggests that since tidal ranges and salinity gradients are small, these systems are dominated by the completion between thermal stratification and wind mixing [59, 60]. Both the Severn and South Rivers displayed considerable heating during the mid-summer for 2010 and 2011. A considerable percentage of the spatiotemporal volume for these rivers during 2010 and 2011 were at or above the critical temperature of 29 °C. Severe temperatures, such as those found in these rivers, especially in Round Bay of the Severn River, maybe a leading cause for the

http://dx.doi.org/10.1016/j.heliyon.2016.e00157

significant reduction in submerged aquatic vegetation in this area over the last two decades.

Some researchers have suggested Coriolis, or even seiching mechanisms to explain water mass intrusions along the western side of the Chesapeake Bay and into the tributaries [63, 64]. However, several problems exist when using these mechanisms to explain hypoxia in the tributaries of the Lower Western Shore of Maryland in the upper Chesapeake Bay. To begin with, the small-scale physics of these tributaries does not lend itself to these physical forcing mechanisms. In particular, Lee et al. [63] used the ChesROMS model to explain increases in hypoxia along the western edge of the Chesapeake Bay. The concept involved wind forcing and a Coriolis mechanism to drive higher nutrients and therefore larger Chlorophyll a values. The main problem invoking this mechanism in the upper bay is that in this area, the Rossby radius of deformation is too small for Coriolis to be an important physical factor. On the other hand, seiching has been shown to occur in the lower Chesapeake Bay that may be related to low oxygen water mass intrusions [64].

Again, the Severn and South Rivers also differ from their large tributary counter parts. Both the York and Rappahannock Rivers show signs of low oxygen intrusions from the main-stem into the mouth of these rivers [65, 66]. However, the Seven and South Rivers do not appear to exhibit this behavior despite research that suggests that seiching in the Lower Bay due to the East-West component of the wind can create a whole Chesapeake Bay effect [67, 68]. The major difference appears to be the bathymetry. The major tributaries have true rivers entering with large thalwegs that connect to the main-stem channel of the Chesapeake Bay at depths much lower than their Northern small tributary counterparts., The deeper thalweg depths make low oxygen intrusions by seiching a real possibility in the lower bay. In contrast, the shallow sills at the mouth of the South and Severn Rivers would generate enough turbulence to explain the well-mixed conditions in these areas even during seiching events, preventing low oxygenated water from penetrating deep into these estuaries.

The results of the spatiotemporal hypoxia models illustrate important similarities and differences between the Severn and South Rivers. Although the initial timing and location of hypoxia are similar, hypoxia and especially anoxia appears to be stronger and last longer in the Severn River. We hypothesize that the main reason for this is rooted in wind efficiency. The Severn River has high bluffs in the upper reaches of the river effectively blocking the wind. Conversely, the South River has low-lying bluffs allowing for efficient wind mixing. In the case of the South River wind mixing can get all the way to the bottom of the tributary, where in the Severn it usually can only get down to about 3-meters. This creates a hypoxic fencing situation in both rivers as hypoxia and anoxia are recognized in the vertical,

http://dx.doi.org/10.1016/j.heliyon.2016.e00157

horizontal, and temporal domains. This concept of hypoxic fencing or squeezing is illustrated in Fig. 14. In this model of hypoxic fencing, the surface of the water column heats up above 28 °C, while severe hypoxic and anoxic waters grow from the bottom creating vertical hypoxic squeezing. During this vertical hypoxic squeezing, the livable potion of the water column is probably the main cause of the large 2010 fish kill in the upper Severn River during July of 2010. In this case, anoxia coupled with a North-westerly wind during ebb tide significantly reduced the livable portion of this narrow section of the river leading to an estimated 100,000 menhaden fish kill. Hypoxic squeezing can also occur in other dimensions, as up-stream growth of hypoxia an anoxia can cause the creation of a lateral hypoxic fence. In this case, above the fence in the upper estuarine reaches, the hypoxia has reached more than half way up the water column. Downstream sections have healthier oxygen levels throughout the water column. This leaves non-mobile living resources stranded behind the fence such as SAV and oysters. Temporal fencing can occur as hypoxia grows and decays over the summer period leading to points in time where the habitable area has decreased significantly but re-opens after some period.

5. Conclusion

This research has shown that the South and Severn Rivers exhibit hypoxia dynamics totally independent of the direct influence of the deep-water hypoxia dynamics of the Chesapeake Bay. The use of the Direct Volume Rendering Technique for modeling real data, allowed us the ability to dissect the water column into slices to evaluate the life cycle of hypoxia in multiple sub-watersheds of the Chesapeake Bay. This provided a detailed visualization of the spatiotemporal data and therefore a more complete resolution of the biophysical processes in these estuarine environments. Modeling real data with a smaller spatiotemporal

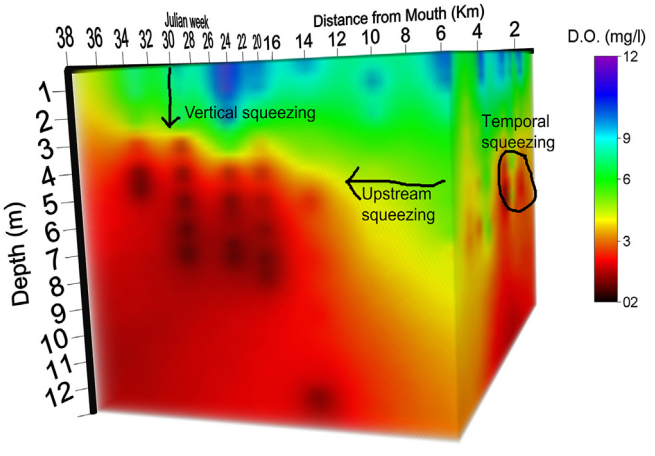

Fig. 14. Spatiotemporal model of hypoxic squeezing.

http://dx.doi.org/10.1016/j.heliyon.2016.e00157

scales assists in understanding the extent and duration of hypoxic and anoxic events. The importance of using the DVR modeling can show water quality details and physical structure that could not be seen in larger scale models. This is extremely important for localized watershed management, because if the main stem of the Chesapeake Bay hypoxia is remediated to healthy conditions, this will not translate to the South and Severn estuarine systems. The remediation of healthier dissolved oxygen for these sub-watersheds must be performed internally.

Declarations

Author contribution statement

Andrew C. Muller, Diana L. Muller, Arianna Muller: Conceived and designed the experiments; Performed the experiments; Analyzed and interpreted the data; Contributed reagents, materials, analysis tools or data; Wrote the paper.

Funding statement

This research did not receive any specific grant from funding agencies in the public, commercial, or not-for-profit sectors.

Competing interest statement

The authors declare no conflict of interest.

Additional information

No additional information is available for this paper.

Acknowledgements

We would like to thank Dr. Pierre Henkart of Severn Riverkeeper Inc, USNA midshipman of the Oceanography Department, Dr. Paula Frohring, Keaghan Muller, and Daisy Muller for their insight and assistance in both field and laboratory.

References

[1] M.A. Mallin, V.L. Johnson, S.H. Ensign, Comparative impacts of Stormwater runoff on water quality of an urban and rural stream, Environ. Monit. Assess. 159 (1) (2009 December) 475–491.

[2] T.A. MacPherson, L.B. Cahooh, M.A. Malin, Water column oxygen demand and sediment oxygen flux: Patterns of oxygen depletion in tidal creeks, Hydrobiologia 586 (1) (2007 April 17) 335–3481.

http://dx.doi.org/10.1016/j.heliyon.2016.e00157

[3] A.C. Muller, D.L. Muller, Analysis of nodal point pollution, variability and sustainability in mesohaline tidal creeks, Marine Poll. Bull. 85 (1) (2014 August 15) 204–213.

[4] R. Diaz, R. Rosengerg, Spreading dead zones and consequences for marine ecosystems, Science 321 (5891) (2008 August 15) 926–929.

[5] T.E. Whitledge, Executive Summary Nationwide review of oxygen depletion and eutrophication in estuarine and coastal waters, Technical Upton: NOAA, DOE, and Brookhaven National Lab, Ocean Assessment Division, (1985) Report No.: BNL-37144, ON:DE89012387.

[6] S.A. Gerlach, Nitrogen, phosphorus, plankton and oxygen deficiency in the German Bight and in Kiel Bay, Final Sonderheft, Kieler Meeresforschungen (1990 January) Report No. 7.

[7] Committee on Environmental and Natural Resources (CENR) CoEaNR, Integrated assessment of hypoxia in the northern Gulf of Mexico National Science and Technology, Council on Environment and Natural Resources, Washington D.C, 2000.

[8] R.J. Diaz, Overview of hypoxia around the world, J. Environ. Qual. (2001 January 30).

[9] J. Borum, T. Pedersen, M. Greve, A. Frankovich, J.C. Zieman, W. Fourqurean, C.J. Madden, The potential role of plant oxygen and sulphide dynamics in die-off events of the tropical seagrass, *Thalassia testudinium*, J. Ecol. 2005 (93) (2016) 148–158.

[10] D.L. Breitburg, Effects of hypoxia and the balance between hypoxia and enrichment on coastal fishes and fisheries, Estuar. Coast. 25 (4b) (2002 August) 767–781.

[11] R.J. Diaz, R. Rosenberg, Marine benthic hypoxia: A review of its ecological effects and the behavioral responses of benthic macrofauna, Oceanogr. Mar. Biol.: An Annual Review 33 (1995) 245–303.

[12] N.N. Rabalais, D.E. Harper, Studies of benthic biota in areas affected by moderate severe hypoxia, Technical Galveston: Louisiana Universities Marine Consortium, Texas A&M University, NOAA, Coastal Ocean Program Office, Sea Grant Program, (1991) Report No.: TAMU-SG-92-109.

[13] D.M. Dauer, A.J. Rodi Jr., J.A. Ranasinghe, Effects of low dissolved oxygen events on the macrobenthos of the lower Chesapeake Bay, Estuar. Coast. 15 (3) (1992 September).

http://dx.doi.org/10.1016/j.heliyon.2016.e00157

[14] ORCA, Red Tides: A summary of issues and activities in the United States Final, Silver Spring: NOAA, Office of Ocean Resources Conservation and Assessment, (1992) Report No.: ORCA 1.

[15] J.M. Burkholder, H.B. Glasgow Jr., C.W. Hobbs, Fish kills linked to a toxic ambush predator dinoflagellate: distribution and environmental conditions, Mar. Ecol. Prog. Ser. 124 (1995) 43–61.

[16] J.M. Burkholder, M.A. Mallin, H.B. Glasgow Jr., Fish kills, bottom water hypoxia and the toxic Pfiesteria complex in the Neuse River and Estuary, Mar. Ecol. Prog. Ser. 179 (1999) 301–310.

[17] S.B. Bricker, C.G. Clement, D.E. Pirhalla, S.P. Orlando, D.R.G. Farrow, National Estuaries Estuarine Eutrophication Assessment, Effects of nutrient enrichment in the nation's estuaries, Silver Spring: NOS Special Projects Office, NOAA, 1999.

[18] S.B. Bricker, C.J. Stevenson, Nutrients in coastal waters, a dedicated issue, Estuaries 19 (2B) (1996) 337–500.

[19] S.W. Nixon, M.E.Q. Pilson, Nitrogen in estuarine and coastal marine ecosystem, In: E.J. Carpenter, D.G. Capone (Eds.), Academic Press, New York, 1983.

[20] Y. Zhou, D. Scavia, A. Michalak, Nutrient loading and meteorological conditions explain interannual variability of hypoxia in Chesapeake Bay, Limnol. Oceanogr. 59 (2) (2014) 373–384.

[21] R. Biggs, Susceptibility of United States Estuaries to anthropogenic impacts, Washington D.C.: Office of Marine and Estuarine Protection, EPA, 1986.

[22] C.L. Dybas, Dead zones spreading in world oceans, Bioscience 55 (2004) 634–658.

[23] J.D. Hagy, W.R. Boyton, C.W. Keefe, K.V. Wood, Hypoxia in Chesapeake Bay, 1950-2001: long-term change in relation to nutrient loading and river flow, Estuaries 27 (2004) 634–638.

[24] C.B. Officer, R.B. Biggs, J.L. Taft, L.E. Cronin, M.A. Tyler, W.R. Boynton, Chesapeake Bay Anoxia: origin, development, and significance, Science 223 (1984).

[25] M.R. Williams, S. Filoso, B. Longstaff, W.C. Dennison, Long-term trends of water quality and biotic metrics in Chesapeake Bay: 1986-2008, Estuar. Coast. 33 (2010) 1279–1299.

[26] Muller and Muller, Forecasting future estuarine hypoxia using a wavelet based neural network model 96 (2) (2015) 314–323.

 http://dx.doi.org/10.1016/j.heliyon.2016.e00157

[27] J. Testa, M. Kemp, Spatial and temporal patterns of winter-spring oxygen depletion in Chesapeake Bay bottom water, Estuar. Coast. 37 (6) (2014) 1432–1444.

[28] D.F. Boesch, R.B. Brinsfeld, R.E. Magnien, Chesapeake Bay Eutrophication: Scientific Understanding, Ecosystem restoration, and challenges for agriculture, J. Environ. Qual. 30 (2) (2001) 303–320.

[29] J.N. Boyer, P. Sterling, R.D. Jones, Maximizing information from a water quality monitoring network through visualization technique, Estuar. Coast. Shelf Sci. 50 (2000) 39–48.

[30] W.H. Jimenez, W.T. Correa, C.T. Silva, A.M. Baptista, Visualizing spatial and temporal variability in coastal observatories, Proceedings of the 14th IEEE Visualization 2003 (VIS'03), October 22-24 2003, pp. 75.

[31] Y. Shen, J.R. Crouch, J.A. Austin, M.S. Dinniman, Interactive visualization of regional ocean modeling system, In Proceedings of the IASTED International Conference of Graphics and Visualization in Engineering, 2007, pp. 74–82. http://dl.acm.org/citation.cfm?id=1712936&picked=prox.

[32] K. Gaither, R.J. Moorhead, S. Nations, D. Fox, Visualizing ocean circulation models through virtual environments, In IEEE Computer Graphics and Applications 17 (1) (1997) 16–19.

[33] A. Bever, M. Friedrich, C. Friedrichs, M. Scully, L.W.J. Lanerolle, Combining observations and numerical model results to improve estimates of hypoxic volume within the Chesapeake Bay, USA, J. Geophys. Res. Oceans 118 (2013) 1–21.

[34] T.S. Elsdon, S.D. Connell, Spatial and monitoring of coastal water quality: Redefining the way we consider, gather and interpret patterns, Aquat. Biol. 5 (2009) 157–166.

[35] L. Zaikowski, K.T. McDonnell, R.F. Rockwell, F. Rispoli, Temporal and spatial variations in water quality on New York South Shore tributaries: Carmens Parchague and Swan Rivers, Estuar. Coast. 31 (1) (September 14, 2007) 85–100.

[36] A.H. Lanoux, H. Etcheber, S. Schmidt, A. Sottolichio, G. Chabaud, M. Richard, G. Abril, Factors contributing to hypoxia in a highly turbid, macrotidal estuary (the Gironde, France), Env. Sci. Process. Impact. 15 (2013) 685–695.

[37] V. Nikolic, S.P. Simonovic, D.B. Milicevic, Analytical support for integrated water resources management: a new method for addressing spatial and temporal variability, Water Resour. Manag. 27 (2016) 401–417.

http://dx.doi.org/10.1016/j.heliyon.2016.e00157

[38] R. Murphy, E. Perlman, W. Ball, F. Curriero, Water-Distance-Based Kriging in Chesapeake Bay, J. Hydrol. Eng. (2014) 05014034.

[39] M. Chehata, D. Jasinski, M.C. Monteith, W.B. Samuels, Mapping three-dimensional water quality data in the Chesapeake Bay using geostatistics, J. Am. Water Resour. Assoc. (JAWRA) 43 (3) (2007).

[40] E. Urquhart, M.J. Hoffman, R. Murphy, B. Zaitchik, Geospatial interpolation of MODIS derived salinity and temperature in the Chesapeake Bay, Remote Sens. Environ. 135 (2013) 167–177.

[41] S. Rouhnani, D.E. Myers, Problems in space-time kriging of geohydrological data, Math. Geol. 22 (5) (1990) 611–623.

[42] A.W. Marcus, M.S. Kearney, Upland and coastal sediment sources in a Chesapeake Bay estuary, Ann. Assoc. Am. Geogr. 81 (3) (1991) 408–424.

[43] The Visualization Handbook, In: C.R. Johnson, C. Hansen (Eds.), Elsevier, Oxford, 2004.

[44] W. Mak, Y. Wu, M. Chan, Visibility-aware direct volume rendering, J. Comput. Sci. Technol. 25 (2) (2011) 217–228.

[45] S.P. Callahan, J.H. Callahan, C.E. Scheidegger, C.T. Silva, Direct volume rendering, Comput. Sci. Eng. 1 (2016) 88–92.

[46] K. Engle, M. Krauss, T. Ertl, High quality pre-integrated volume rendering using hardwire-accelerated pixel shading, Proceeding of the EG/SIGGRAH workshop on graphic hardwire, 2001, pp. 9–16.

[47] R. Drebin, P. Carpenter, P. Hanrahan, Volume rendering, Comput. Graphics 22 (4) (1988) 65–74.

[48] Voxler 3 Golden, Quick Start Guide, Golden Software Inc, 2012, 2016.

[49] USEPA, Ambient water quality criteria for dissolved oxygen, water clarity and chlorophyll a for the Chesapeake Bay and its tidal tributaries, Technical Report Annapolis, EPA, 2008, 2016.

[50] Association of Limnology and Oceanography, The Venice System for the classification of marine waters according to salinity 3 (3) (1958) 346–347.

[51] R.A. Batiuk, D.L. Breitburg, R.J. Diaz, T.M. Cronin, D.H. Secor, G. Thursby, Derivation of habitat-specific dissolved oxygen criteria for Chesapeake Bay and its tidal tributaries, J. Exp. Mar. Biol. Ecol. 381 (1) (2009) 204–215.

[52] K.A. Moore, D.J. Wilcox, R.J. Orth, Analysis of the abundance of submerged aquatic vegetation communities in the Chesapeake Bay, Estuaries 23 (2000) 115–127.

 http://dx.doi.org/10.1016/j.heliyon.2016.e00157

[53] K.A. Moore, J.C. Jarvix, Environmental factors affecting recent summertime eelgrass diebacks in the Lower Chesapeake Bay: Implications for long-term persistence, J. Coastal Res. (2008) 135–147.

[54] K.A. Moore, E.C. Shields, D.B. Parrish, R.J. Orth, Eelgrass survival in two contrasting systems: role of turbidity and summer water temperatures, Mar. Ecol. Prog. Ser. 448 (2012) 247–258.

[55] USEPA Appendix, Ambient water quality criteria for dissolved oxygen water clarity and chlorophyll a for the Chesapeake Bay and its tidal tributaries, (2007) , pp. C-2.

[56] R. Batiuk, et al., Derivation of habitat specific dissolved oxygen criteria for Chesapeake Bay and its tidal tributaries, J. Exp. Mar. Biol. Ecol. (2009) 381.

[57] P. Tango, R. Batiuk, Deriving water quality standards for Chesapeake Bay, J. Am. Water Resour. Assoc. (2013 September) 1–18.

[58] L.W. Harding, R. Batiuk, T.R. Fisher, C.L. Gallegos, T.C. Malone, W.D. Miller, M.R. Mulholland, H.W. Paerl, E.S. Perry, P. Tango, Scientific bases for numerical chlorophyll criteria in Chesapeake Bay, Estuar. Coast. (June 2014) 134–148.

[59] J. Hardisty, Estuaries Modeling and monitoring the physical system, Wiley-Blackwell, 2007, 2016, pp. 176.

[60] W.M. Cameron, D.W. Pritchard, The Sea Estuaries, In: M.H. Hill (Ed.), 2nd ed., John Wiley and Sons, New York, 1963.

[61] D. Pritchard, Estuarine circulation patterns, Proceedings of the American Society of Civil Engineers 81 (1955) 711–717.

[62] R. Murphy, W.M. Kemp, W.P. Ball, Long-term trends in Chesapeake Bay seasonal hypoxia: stratification and nutrient loading, Estuar. Coast. 37 (8) (2011) 1293–1309.

[63] L. Fernandes, G.N. Nayak, D. Iilangovan, D.V. Borole, Accumulation of sediment, organic matter and trace metals with space and time, in a creek along Mumbai coast, India, Estuar. Coast. Shelf Sci. 91 (2011) 388–391.

[64] Y.J. Lee, W.R. Boynton, Y. Li, Role of late winter spring wind influencing summer hypoxia in Chesapeake Bay, Estuar. Coast. 36 (2013) 683–696.

[65] M.E. Scully, Physical controls on hypoxia in Chesapeake Bay: A numerical modeling study, JGR Oceans 118 (2013) 1239–1256.

[66] W. Reay, Water quality within the York River estuary, J. Coastal Res. SI(57 (2009) 23–39.

 http://dx.doi.org/10.1016/j.heliyon.2016.e00157

[67] W.C. Long, D.S. Rochelle, Hypoxia in Chesapeake Bay tributaries: Worsening effects on microbenthic community structure in the York River, Estuar. Coast. 32 (2009) 287–297.

[68] W.S. Chung, W. Boicourt, Resonant seiche motion in the Chesapeake Bay, JGR Oceans 94 (C2) (1989) 2105–2110.

 http://dx.doi.org/10.1016/j.heliyon.2016.e00157